Biol Fertil Soils (2005) 42: 24–30
DOI 10.1007/s00374-005-0866-3

ORIGINAL PAPER

Liesbet Cockx · Marc Van Meirvenne · Georges Hofman

Characterization of nitrogen dynamics in a pasture soil by electromagnetic induction

Received: 7 April 2004 / Revised: 11 March 2005 / Accepted: 11 March 2005 / Published online: 23 April 2005

Abstract The aim of this study was to investigate how electromagnetic induction can be used to improve the characterization of N dynamics in a 1.2 ha pasture. The soil apparent electrical conductivity (ECa) was measured by electromagnetic induction using an EM38DD. At 116 locations, soil samples were taken according to a clustered sampling design, three times during one winter, and analyzed for the NO_3^-–N content in the topsoil (0–60 cm). Management zones were delineated using a fuzzy *k*-means classification of the interpolated ECa measurements. Two ECa zones were found, reflecting mainly differences in soil texture. Since the mean NO_3^-–N content was different for the two ECa zones (24 and 65 kg/ha in November 2002), the residuals were interpolated using stratified simple kriging. This allowed evaluating the NO_3^- dynamics during the winter in both zones; one ECa zone showed a higher risk for NO_3^- losses than the other calling for a site-specific N management. As a validation, NO_3^-–N was interpolated using orinary kriging without stratification. This resulted in similar zones confirming the usefulness of the ECa measurements to assess N-specific management zones, even within small fields.

Keywords Electromagnetic induction · Geostatistics · Management zones · Nitrate dynamics

Introduction

Since NO_3^- leaching is a worldwide concern, an appropriate N management will become essential in future agricultural practices. Methods will be needed to evaluate the NO_3^- variability in space and time. Much of the NO_3^- leached from pastures during the winter originates from the high concentrations of N deposited in urine patches during the grazing season (Ryden et al. 1984). One urine patch can represent local N applications ranging from 400 to 1,200 kg/ha (Addiscot et al. 1991). This N cannot be fully utilized by the grass crop at the end of the growing season, so efforts should be made to minimize the soil mineral N in late autumn. Site-specific N management adjusts to the different NO_3^- dynamics within one field, with the aim to decrease the amount of leached NO_3^-. The NO_3^-–N content of pastures is characterized by a high spatial variability (Bogaert et al. 2000). Spatial variability in NO_3^- within a grazed pasture occurs principally because of the presence of urine and, to a lesser extent, of dung patches. This spatial variability alters each time the field is grazed. Variability in soil properties within a field can also affect the magnitude of soil processes such as nutrient accumulation and loss. This paper focuses on the NO_3^-–N variability that can be explained by soil differences. To reduce the number of samples and consequently the cost of a classical sampling scheme, a mobile sensor system based on the principle of electromagnetic induction can be used to characterize soil variability at within-field scale. Electromagnetic induction sensors measure the apparent electrical conductivity (ECa) of a soil and are widely applied to characterize field variability for application to precision agriculture (Rhoades et al. 1999). It has been found that ECa measurements are related to a number of soil properties, like soil texture (McNeill 1980a), soil water content (Sheets and Hendrickx 1995) and exchangeable Ca and Mg (McBride et al. 1990). Electrical conductivity is also being studied as an indirect measure for NH_4^+ and K^+ in animal slurries (Stevens et al. 1995). Laboratory measurements of $EC_{1:1}$ (1:1 soil to water solution) have been used to estimate the soil NO_3^-–N content (Smith and Doran 1996). Zhang and Wienhold (2002) demonstrated the use of a portable EC meter to detect changes in soil inorganic N status in non-saline, carbonates-free soil. Electromagnetic conductivity methods have been used to detect specific mobile ions that are associated with animal waste (Eigenberg et al. 1998). High correlations were obtained with profile weighted ECa measurements of an EM38 in horizontal

L. Cockx (✉) · M. Van Meirvenne · G. Hofman
Department of Soil Management and Soil Care,
Ghent University,
Coupure 653,
9000 Ghent, Belgium
e-mail: liesbet.cockx@ugent.be

orientation (ECa to about 75 cm) and soil NO_3^-–N in the surface 0–23 and 23–46 cm soil layers throughout the growing season in corn field (Eigenberg et al. 2002).

The aim of this study was to investigate how electromagnetic induction can be used to characterize differences in NO_3^- dynamics within one field. We did not intend to predict the absolute amount of NO_3^-–N in the pasture by means of electromagnetic induction.

Materials and methods

The study area was a flat cattle pasture of 1.2 ha in Lovendegem, Belgium. According to the Belgian soil map, the topsoil texture was silty-clayey sand. The pasture has been treated with two types of fertilizers: liquid cow slurry applied early March 2002 at a rate equivalent to 120 kg N ha^{-1} and a mineral fertilization applied as NH_4NO_3 (27% N) in April, May and June 2002, resulting in a total of 216 kg N ha^{-1}. The field was sampled according to a clustered sampling design at 116 locations (Fig. 1a). Soil samples were taken at three depths (0–10, 10–30 and 30–60 cm) on 4 November 2002, 27 January 2003 and 12 March 2003. All these samples were analyzed for the NO_3^-–N content; in the top 30 cm, the soil was analyzed by a continuous flow auto analyzer (Kalra and Maynard 1991). The subsoil was analyzed with a NO_3^- specific electrode (Orion 1991). Here, we have considered only the total NO_3^-–N content of 0 to 60 cm topsoil.

In November 2003, the ECa of the pasture was measured by a non-invasive and non-destructive electromagnetic induction method. We used a commercially available instrument, the EM38DD, manufactured by Geonics Ltd., Ontario. The EM38DD is a dual dipole instrument and consists out of two identical EM38s positioned perpendicular to each other: one instrument orientated horizontally and the other one vertically. The EM38DD measures simultaneously the ECa in the two orientations, and each orientation has a different depth response profile. The vertical orientation (EC_v) receives a dominant influence of deeper (30–60 cm) soil layers, whereas the horizontal orientation (EC_h) has a major influence of the near-surface soil layers (McNeill 1980b). The EM38DD was attached to an all-terrain vehicle (ATV) and connected with a field computer and a global positioning system (GPS). The ATV was driven along parallel lines with an interval of 5 m, and EC_h and EC_v measurements were taken simultaneously every second (Fig. 1b).

Continuous maps of both EC_v and EC_h were obtained using ordinary kriging (OK), based on the spatial autocorrelation among data whereby a variogram is used to model the spatial variability of these data. Estimates of the variable at unsampled locations $Z^*(x_0)$ were calculated using the basic linear regression equation (Goovaerts 1997):

$$Z^*(x_0) - m(x_0) = \sum_{\alpha=1}^{n(x_0)} \lambda_\alpha(x)[Z(x_\alpha) - m(x_0)] \qquad (1)$$

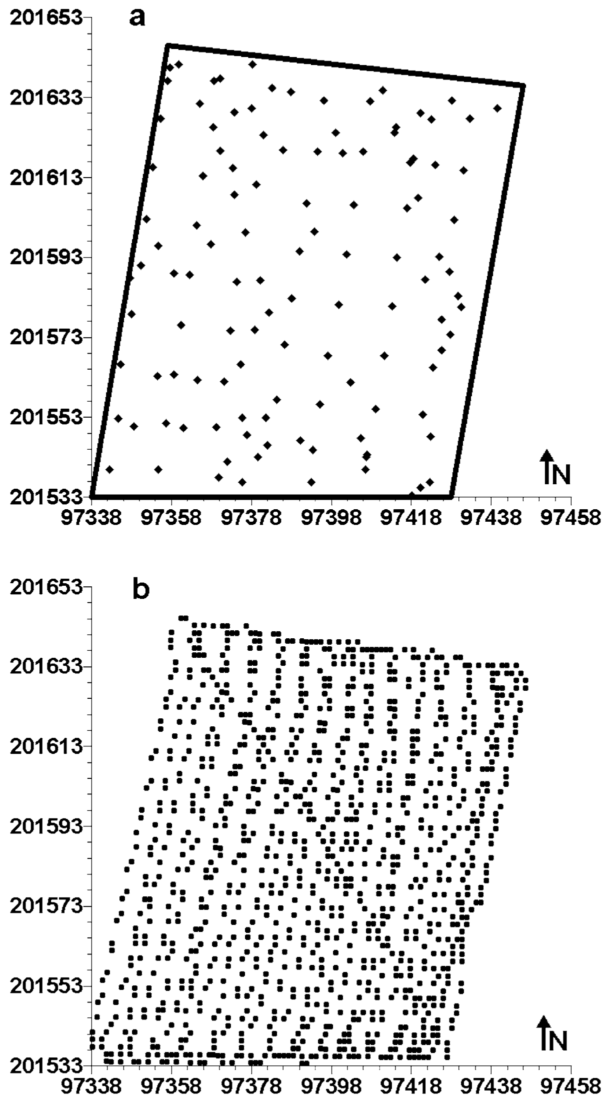

Fig. 1 Indication of the sampling sites (**a**) and the ECa measurements (**b**) (the coordinates are expressed in meters, conform the Lambert 72 projection used in Belgium)

where $\lambda_\alpha(x)$ is the unknown weight assigned to the observation $Z(x_\alpha)$, $m(x_0)$ and $m(x_\alpha)$ are the expected values of $Z(x_0)$ and $Z(x_\alpha)$, respectively, and the number of data used in the interpolation is $n(x_0)$, being the data located within a given neighbourhood around x_0. The weight $\lambda_\alpha(x)$ was obtained by solving the kriging algorithm, in which the variogram model was used to convert the spatial distances into variogram values. Ordinary kriging requires the mean $m(x_0)$ to be stationary within the neighbourhood around x_0. The interpolated EC_v and EC_h values were used as input for a fuzzy *k*-means classification to create management zones. A fuzzy *k*-means classification allows allocating each individual as a member of each class (Triantifilis et al. 2003). The method minimizes the multivariate within class variance, and consequently, individuals classified to the same class have similar attributes (McBratney and de Gruijter 1992). Therefore, ECa zones reflected differences in soil condition like soil texture and moisture, the most important factors affecting the ECa of non-saline soils.

In addition, the NO_3^-–N measurements were interpolated using stratified simple kriging (SK) using the ECa zones as strata. Simple kriging requires the global mean to be known and stationary over the entire study area. Therefore, for SK, Eq. 1 becomes:

$$Z^*(x_0) - m = \sum_{\alpha=1}^{n(x_0)} \lambda_\alpha(x)[Z(x_\alpha) - m] \qquad (2)$$

where m is the stationary mean. In the situation where two or more zones (strata) exist within a study area, each with a different mean, the observations can be transformed to residuals with zero mean by subtracting their local means. The residuals can then be interpolated using a variogram of the residuals, after which the local means are added. This procedure was followed to include the ECa zones into the mapping of NO_3^-–N at the three sampling times. Comparing these maps, the NO_3^- dynamics of the pasture could be interpreted by considering two periods: from 3 November till 27 January and from 28 January till 12 March. The ratio obtained by dividing the NO_3^-–N content of the first period by the NO_3^-–N content of the second period indicated the NO_3^-–N dynamics. If this ratio was larger than 1, NO_3^-–N was lost; otherwise, it accumulated.

Finally, we interpolated the NO_3^-–N content at the three sampling times independently from the ECa measurements by OK. These three NO_3^-–N maps were used in a fuzzy *k*-means classification to create NO_3^- zones. To validate the accuracy of the interpolation methods, a cross-validation (leave-one-out method) was performed. The mean square estimation error (MSEE) was used to compare the two interpolation methods:

$$\mathrm{MSEE} = \frac{1}{n}\sum_{\alpha=1}^{n} \{z^*(x_\alpha) - z(x_\alpha)\}^2 \qquad (3)$$

where the number of observed values $z(x_\alpha)$ (α=1,...,n) is n and $z^*(x_\alpha)$ are the estimated values at the same locations. The relative improvement (RI) of precision was calculated:

$$\mathrm{RI} = 100\% \frac{(\mathrm{MSEE_{OK}} - \mathrm{MSEE_{SK}})}{\mathrm{MSEE_{OK}}} \qquad (4)$$

where $\mathrm{MSEE_{OK}}$ and $\mathrm{MSEE_{SK}}$ were the MSEE for the OK using NO_3^- data only and the SK of NO_3^- data involving the ECa zones, respectively. If RI is positive, the precision of the SK method is superior to OK.

Results and discussion

The OK-interpolated EC_v and EC_h maps are given in Fig. 2. Three corners of the field showed increased ECa values, and these areas corresponded to muddy and stony parts representing the drinking place and the entrances/exits to the field. Since these areas represent human-induced artifacts, they were not considered further. The central and lower parts of the field showed low ECa values, whereas the upper left part was mainly characterized by intermediate ECa values. EC_v and EC_h displayed similar patterns except for the upper left corner where EC_v was larger than EC_h, indicating a more heterogeneous soil.

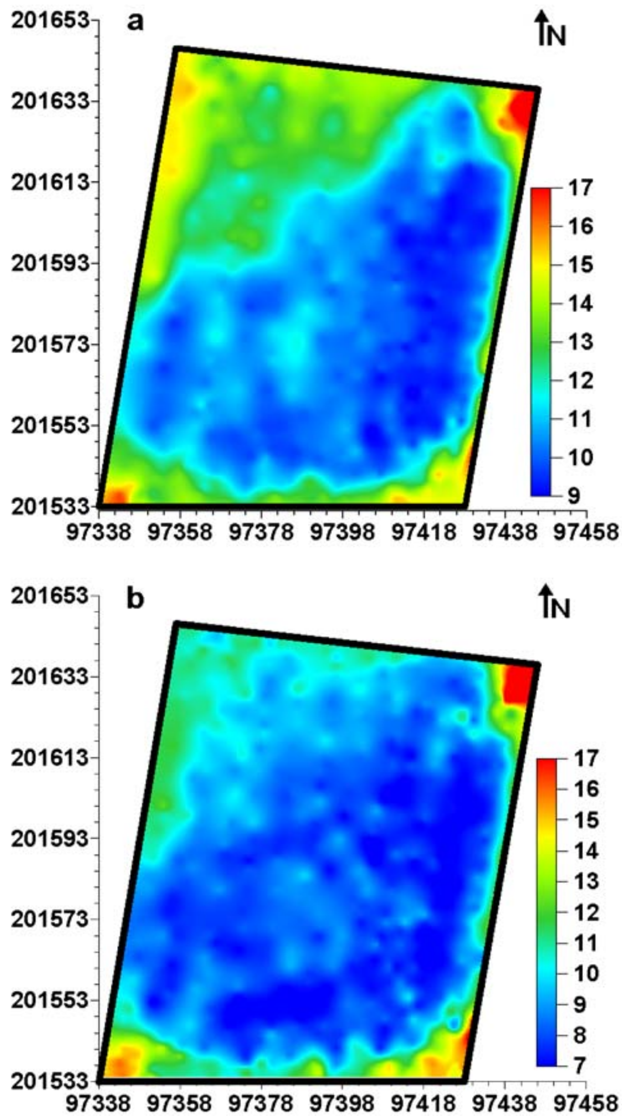

Fig. 2 Interpolated maps (ECa units are mS m^{-1}) of EC_v (**a**) and EC_h (**b**) (the coordinates are expressed in meters, conform the Lambert 72 projection used in Belgium)

The fuzzy *k*-means classification confirmed our observations; the field was divided into two zones: zone 1 with low ECa values and zone 2 with higher ECa values (Fig. 3a). A texture analysis confirmed the differences in ECa (Fig. 3b). The mean profile of zone 1 had a homogeneous sandy texture, with a sand content ranging from 79 to 87% down to 90 cm. The mean profile within zone 2 also showed a sandy topsoil (70% sand fraction) but with a clear reduction in sand content with depth (to about 60%). Moreover, with the consequent increase in clay and silt contents, zone 2 was noticeably wetter during fieldwork. Although the absolute

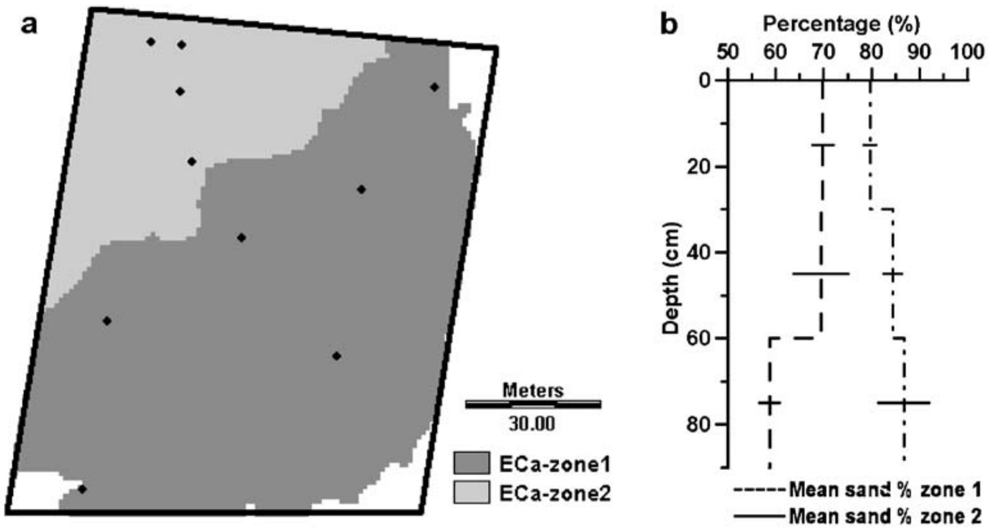

Fig. 3 Fuzzy *k*-means classification based on ECa maps with indication of the texture samples (**a**) and mean sand content in the ECa zones (**b**) (the *error bars* depict the standard deviations of the mean)

ECa values might fluctuate over time, spatial patterns of ECa generally remain constant (Sudduth et al. 2001), resulting in stable management zone delineations.

The NO_3^-–N data at the three sampling times were stratified according to the two ECa zones; the relative statistical analysis is reported in Table 1. On average, zone 1 contained higher NO_3^-–N concentrations with smaller coefficients of variation than zone 2. One would expect a lower NO_3^-–N content in ECa zone 1 resulting in lower conductivities. However, differences in soil texture often influence the ECa much more than small differences in nutrient concentrations (Heiniger et al. 2003). If ECa changes due to one soil property are much larger than those to other factors, then ECa is mainly determined by that dominant factor (Sudduth et al. 2003). This means that the texture difference between the zones masked the effect of a different NO_3^-–N content in these zones.

After subtracting the mean values from the observations, the variograms of the pooled residuals were calculated and modeled (Fig. 4). For the three sampling times, the semivariance $\gamma(h)$ at lag distances h was defined by a nugget effect C_0 and a spherical model:

$$\gamma(h) = \begin{cases} C_0 + C_1 \times \left[1.5\frac{h}{a} - 0.5\left(\frac{h}{a}\right)^3\right], & \text{if } 0 < h \leq a \\ C_0 + C_1, & \text{if } h > a \end{cases} \quad (5)$$

Table 1 Descriptive statistics of the soil NO_3^-–N content, stratified into two ECa zones

	4 November 2002		27 January 2003		12 March 2003	
	Zone 1	Zone 2	Zone 1	Zone 2	Zone 1	Zone 2
Mean (kg/ha)	65	24	29	16	29	17
Minimum (kg/ha)	11	4	5	4	12	2
Maximum (kg/ha)	290	128	97	109	61	39
CV[a] (%)	90	107	62	115	40	47

[a]*CV*: Coefficient of variation = (standard deviation/mean)×100

where C_1 is the sill and a is the range (Fig. 4). At the end of the winter period, the variograms of the NO_3^-–N residuals displayed a trend to shorter ranges and a larger relative nugget effect $\left[\mathrm{RNE}\,(\%) = \frac{C_0}{C_0+C_1} \times 100\right]$. With time, the NO_3^-–N content did not only decrease but also the NO_3^- variability was less structured and occurred over shorter distances. This implies that gradually, the deterministic mean became a more reliable predictor.

Then SK of the NO_3^-–N residuals was performed, resulting in NO_3^-–N maps for the three sampling times (Fig. 5). A clear separation line between both zones appeared due to the stratification. In November, the highest values were found from the bottom left (field entrance) to the top right (drinking place) of Fig. 5a, corresponding to a preferential walking path of the cows. This can be related to the fact that cattle frequently visits certain parts of the field as, for example, water sources (Barrow 1967). In November, the NO_3^-–N content of zone 2 was much lower than in zone 1. This indicated that the textural differences between the ECa zones also influenced the NO_3^-–N content. The homogeneous sandy soils of zone 1 produced less grass biomass than the more clayey zone 2. Consequently, less fertilizer was used by the crop, resulting in higher NO_3^-–N residues. However, it could also be that the cows visited this wetter area less frequently or that denitrification was favoured under the more clayey and wet conditions of zone 2 (Garrett et al. 1992). Fine-textured soils have slower drainage and a greater potential for denitrification. Nevertheless, it was assumed that denitrification was limited by the low winter temperatures. In January, the NO_3^-–N content and variability decreased, but the difference between the zones remained. In March, the map was more homogeneous because the NO_3^-–N content decreased and the variability smoothened. It is clear that the change in NO_3^-–N content between November and January was higher than the change between January and March. The excessive rainfall between the first two sampling periods resulted in increased NO_3^- losses by leaching. Figure 6 shows the histograms of the ratio of the NO_3^-–N content measured in November and

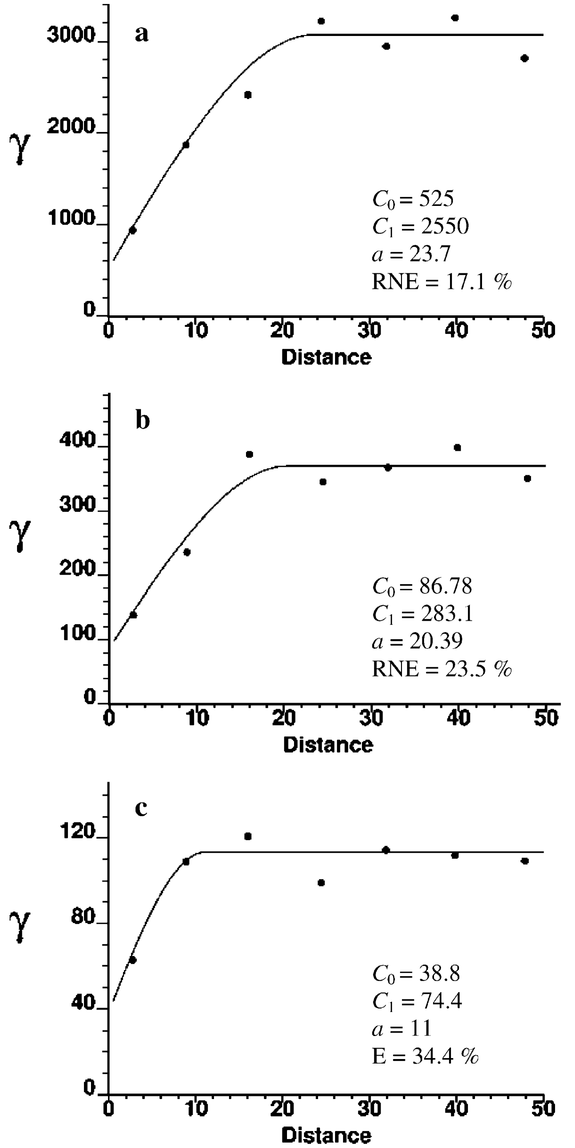

Fig. 4 Variograms of the NO_3^-–N residuals at the three sampling times: 4 November 2002 (**a**), 27 January 2003 (**b**) and 12 March 2003 (**c**); the lag distance in meter is on the *X*-axis, and the semivariogram values γ expressed in (kg NO_3^-–N $ha^{-1})^2$ are at the *Y*-axis. The parameters of the variogram models are also given

the NO_3^-–N content of January, split for the two zones. In zone 1, this ratio was generally higher than 1, indicating large NO_3^- losses in most parts of this zone. In zone 2, the graph is bimodal; although a considerable part of this zone also showed values higher than 1, the highest frequency was for values smaller than 1. It may be concluded that zone 1 has a higher risk for NO_3^- losses than zone 2. The processes of mineralization, (de)nitrification, leaching and immobilization define the soil inorganic N content. They are controlled by soil characteristics as water content, texture, biological activity, cropping and organic matter (Stevenson 1982). Gaines and Gaines (1994) stated that soils with a higher silt and clay content retained more NO_3^-–N than pure sandy soils. Obviously, the sandy zones within this field will require a different N management than the silty-clayey parts.

The RI (Eq. 4) was calculated to evaluate the added value of including the ECa zones in the interpolation of NO_3^-–N. In November, the RI was 1%, in January 12% and in March

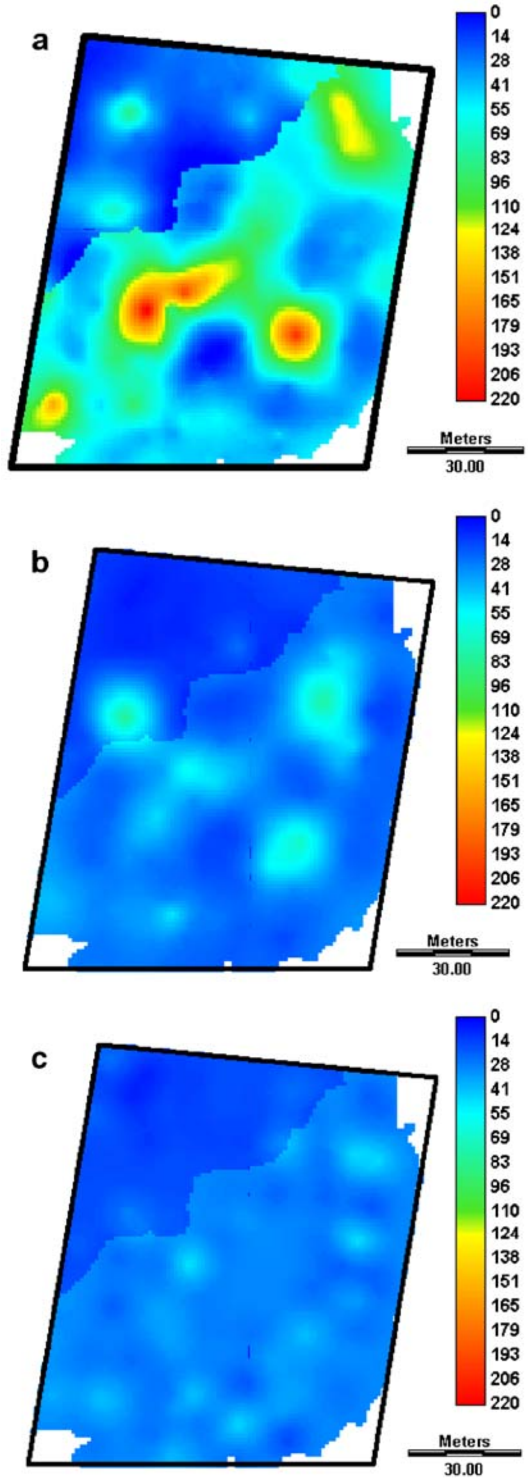

Fig. 5 NO_3^-–N maps in top 60-cm soil (in kg NO_3^-–N ha^{-1}) at three sampling times: 4 November 2002 (**a**), 27 January 2003 (**b**) and 12 March 2003 (**c**)

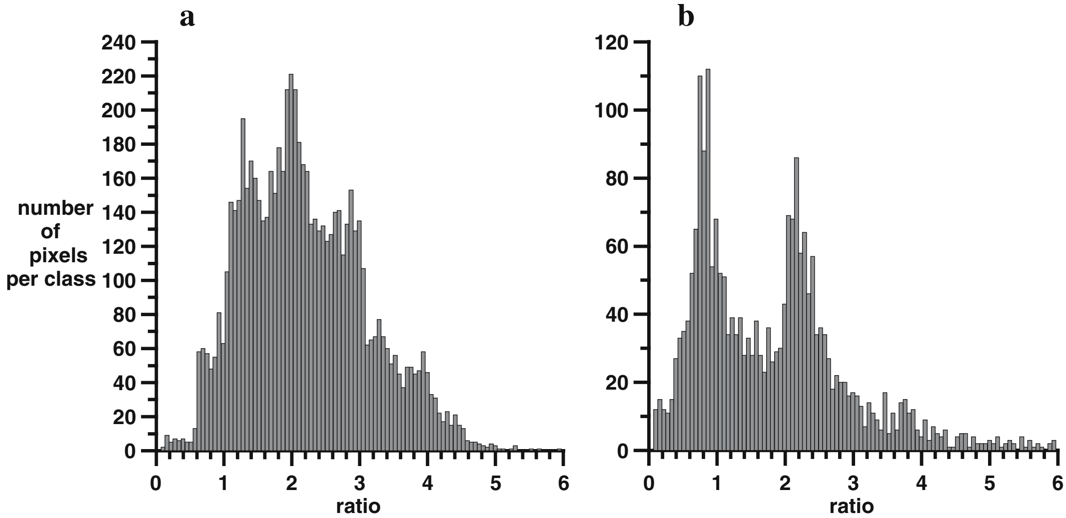

Fig. 6 Histogram (number of pixels per class) of the ratio $\frac{NO_3^- - N \text{ measured in November}}{NO_3^- - N \text{ measured in January}}$ for ECa zone 1 (**a**) and ECa zone 2 (**b**)

5%. These values indicate that taking into account the ECa zones resulted in small to medium improvements in the interpolation of NO_3^-–N. When the NO_3^-–N maps of the three sampling times obtained by OK without the ECa maps were subjected to a fuzzy *k*-means classification with two classes, the resulting pattern (Fig. 7) was very similar to the classified ECa map (Fig. 3). These NO_3^- zones were compared with the ECa zones by cross-tabulation. Individual pixels of the two classifications were compared with each other. Therefore, the ECa zones were taken as reference: 90% of the pixels of ECa zone 1 pixels were classified as NO_3^- zone 1, and 87% of the pixels of zone 2 were classified as NO_3^- zone 2. Since the NO_3^- zones were formed based on the three sampling times, they show places with similar NO_3^- dynamics. Consequently, the ECa zones represent zones of very similar NO_3^- behaviour, and within this field, electrical conductivity can be used as an indirect measure of the risk of NO_3^- losses.

Our study shows that electromagnetic induction measurements are able to delineate zones with different risks of NO_3^- losses. Consequently, in such conditions, a site-specific N management based on ECa zones can be recommended, even within small fields.

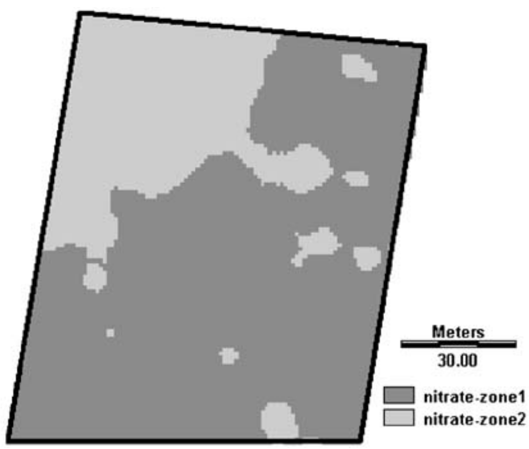

Fig. 7 Fuzzy *k*-means classification based on interpolated NO_3^-–N measurements at three sampling times

Acknowledgements The authors wish to thank Luc Deboosere, Viralbhai Pancholi, Mathieu Schatteman and Preciosa Simons for their support during the field and laboratory work.

References

Addiscot TM, Withmore AP, Powlson DS (1991) Farming, fertilizers and the nitrate problem. CAB International, Wallingford, UK

Barrow NJ (1967) Some aspects of the effects of grazing on the nutrition of pastures. J Aust Inst Agric Sci 33:254–262

Bogaert N, Salomez J, Vermoessen A, Hofman G, Van Cleemput O, Van Meirvenne M (2000) Within-field variability of mineral nitrogen in grassland. Biol Fertil Soils 32:186–193

Eigenberg RA, Korthals RL, Nienaber JA (1998) Geophysical electromagnetic survey methods applied to agricultural waste sites. J Environ Qual 27:215–219

Eigenberg RA, Doran JW, Nienaber JA, Ferguson RB, Woodburry BL (2002) Electrical conductivity monitoring of soil condition and available N with animal manure and a cover crop. Agric Ecosyst Environ 88:183–193

Gaines TP, Gaines ST (1994) Soil texture effect on nitrate leaching in soil percolates. Commun Soil Sci Plant Anal 25:2561–2570

Garrett MK, Watson CJ, Jordan C, Steen RWJ, Smith RV (1992) The nitrogen economy of grazed grassland. Proc -Fert Soc 326:1–32

Goovaerts P (1997) Geostatistics for natural resources evaluation. Oxford University Press, New York

Heiniger RW, McBride RG, Clay DE (2003) Using soil electrical conductivity to improve nutrient management. Agron J 95:508–519

Kalra YP, Maynard DG (1991) Methods manual for forest soil and plant analysis. Inf. Rep. NOR-X-319, Canadian Forest Service, Northern Forestry Centre, Edmonton, AB

McBratney AB, de Gruijter JJ (1992) A continuum approach to soil classification by modified fuzzy k-means with extragrades. J Soil Sci 43:159–175

McBride RA, Gordon AM, Shrive SC (1990) Estimating forest soil quality from terrain measurements of apparent electrical conductivity. Soil Sci Soc Am J 54:290–293

McNeill JD (1980a) Electrical conductivity of soils and rocks. Technical Note TN-5, Geonics Ltd, Ontario, Canada

McNeill JD (1980b) Electromagnetic terrain conductivity measurement at low induction numbers. Technical Note TN-6, Geonics Ltd, Ontario, Canada

Orion Research (1991) Model 93-07 nitrate electrode instruction manual. Orion Research, Boston

Rhoades JD, Chanduvi F, Lesch SM (1999) Soil salinity assessment: methods and interpretation of electrical conductivity measurements. FAO Irrigation and Drainage Paper 57, Food and Agricultural Organization of the United Nations, Rome

Ryden JC, Ball PR, Garwood EA (1984) Nitrate leaching from grassland. Nature 311:50–53

Sheets KR, Hendrickx JMH (1995) Noninvasive soil water content measurement using electromagnetic induction. Water Resour Res 31:2401–2409

Smith JL, Doran JW (1996) Measurement and use of pH and electrical conductivity for soil quality analysis. In: Doran JW, Jones AJ (eds) Methods for assessing soil quality. Soil Sci. Soc. Am. Spec. Publ. 49. SSSA, Madison, WI, pp 169–185

Stevens RJ, O'Bric CK, Carton OT (1995) Estimating nutrient content of animal slurries using electrical conductivity. J Agric Sci (Camb) 125:233–238

Stevenson FJ (1982) Origin and distribution of nitrogen in soil. In: Stevenson FJ (ed) Nitrogen in agricultural soils. Agronomy Monograph Number 22. American Society of Agronomy, Madison, WI, pp 1–42

Sudduth KA, Drummond ST, Kichen NR (2001) Accuracy issues in electromagnetic induction sensing of soil electrical conductivity for precision agriculture. Comput Electron Agric 31:239–264

Sudduth KA, Kitchen NR, Bollero GA, Bullock DG, Wiebold WJ (2003) Comparison of electromagnetic induction and direct sensing of soil electrical conductivity. Agron J. 95:472–482

Triantifilis J, Odeh IOA, Minasny B, McBratney AB (2003) Elucidation of physiographic and hydrogeological features of the lower Namoi valley using fuzzy *k* means classification of EM34 data. Environ Model Softw 18:667–680

Zhang R, Wienhold BJ (2002) The effect of soil moisture on mineral nitrogen, soil electrical conductivity and pH. Nutr Cycl Agroecosyst 63:251–254